JOURNAL OF MATERIALS SCIENCE **39** (2004) 2327– 2334

Formation of intermetallic compound layers in Sn/Au/Sn diffusion couple during annealing at 433 K

T. YAMADA, K. MIURA
Graduate School, Tokyo Institute of Technology, Yokohama 226-8502, Japan
M. KAJIHARA*
Department of Materials Science and Engineering, Tokyo Institute of Technology, Yokohama 226-8502, Japan
E-mail: kajihara@materia.titech.ac.jp
N. KUROKAWA, K. SAKAMOTO
Tyco Electronics AMP Co., Ltd., Kawasaki 214-8533, Japan

The kinetics of the reactive diffusion between Au and Sn was experimentally studied in a metallographical manner. Sn/Au/Sn diffusion couples were prepared by a solid-state diffusion bonding technique and then annealed at 433 K for various times between 1 and 127 h (3.6×10^3 and 4.57×10^5 s) in an oil bath with silicone oil. Due to annealing, intermetallic compound layers consisting of $AuSn_4$, $AuSn_2$ and AuSn are produced at the Au/Sn interface in the diffusion couple. The thickness of the $AuSn_4$ layer is four times greater than those of the $AuSn_2$ and AuSn layers. The ratio of the thicknesses of the compound layers remains constant during annealing. The total thickness l of the compound layers increases with annealing time t. Such a relationship is mathematically described by the equation $l = k(t/t_0)^n$, where t_0 is unity time, 1 s. From the experimental results, the proportionality coefficient and the exponent are determined to be $k = 2.7 \times 10^{-7}$ m and $n = 0.42$, respectively, by a least-squares method. The exponent n is slightly smaller than 0.5. This implies that the grain boundary diffusion partially contributes to the rate-controlling process for the growth of the compound layers.

1. Introduction

Copper-base conductor alloys are widely used in the electronic industry. Such conductor alloys are usually plated with Au in order to improve the corrosion resistance. When the Au-plated conductor alloy is mechanically contacted with a Sn-base solder alloy with or without Pb and then energized under usual service conditions, the ductility and the electrical conductivity of the conductor alloy at the mechanical contact remarkably deteriorate with energization time. The deterioration may be due to diffusion-controlled reactions occurring at the interface between the solder and conductor alloys [1–5].

The reactive diffusion between Au and Sn was experimentally observed by Hannech and Hall using Au/(Sn-Pb) diffusion couples [3]. In their experiment, a commercial flux-cored Sn-28 at% Pb alloy was soldered onto a thin Au layer electrodeposited on an alumina plate to prepare a Au/(Sn-Pb) diffusion couple. The diffusion couples were annealed at temperatures between 353 and 433 K. According to their observations, $AuSn_4$ is formed at the Au/(Sn-Pb) interface during soldering, and then AuSn and $AuSn_2$ are produced at the Au/$AuSn_4$ interface during annealing. Similar observations for the reactive diffusion between Au and Sn are reported also by Keller and Morabito [1, 2, 4] and by Wright [5]. The Au-Sn intermetallic compounds are quite hard and possess high electrical resistivities. The soldering joint usually breaks along the interface between the compound layer and the solder alloy. Thus, the formation of such compounds might be responsible for the mechanical and electrical deterioration of the Au-plated conductor alloy.

The observations by Hannech and Hall [3] indicate that the thickness of the compound layer is mathematically described as a power function of the annealing time. If the growth of the compound layer is controlled by the volume diffusion of the constituent elements in each phase, the thickness of the compound layer should be proportional to the square root of the annealing time. However, the exponent of the power function is smaller than 1/2 and takes different values for the $AuSn_4$, $AuSn_2$

---

*Author to whom all correspondence should be addressed.

and AuSn layers. This means that the volume diffusion is not purely the rate-controlling process and the annealing time dependence of the growth rate is not equivalent for these compound layers. Most of the experiments on the reactive diffusion between Au and Sn have been carried out using the diffusion couples prepared by a soldering technique [1–5]. In such experiments, it is rather difficult to distinguish the growth rate of the compound layer during annealing from the formation rate of the compound layer during soldering. Therefore, the soldering technique may not be suitable to observe the reactive diffusion between solid phases.

In the present study, a solid-state diffusion bonding technique was adopted to examine the kinetics of the reactive diffusion between Au and Sn during annealing. The Sn/Au/Sn diffusion couples prepared by this technique were annealed at 433 K for various times in an oil bath. The microstructure of the annealed diffusion couple was observed in a metallographical manner. The observations may provide certain information about the reactive diffusion occurring at the mechanical contact of the Au-plated conductor alloy with the Sn-base solder alloy during energization.

2. Experimental

Pure Au plates with a size of $10 \times 4 \times 2$ mm^3 were cut by spark erosion from a commercial 100 g rectangular bar of pure Au with purity of 99.99% and then cold rolled to a thickness of 0.06 mm. Sheet specimens with a dimension of $20 \times 7 \times 0.06$ mm^3 were cut from the cold rolled specimens and then separately annealed in evacuated silica capsules at 1273 K for 1 h, followed by air cooling without breaking the capsules. The annealed sheet specimens were chemically polished in nitrohydrochloric acid.

Pure Sn plates with a size of $12 \times 5 \times 2$ mm^3 were prepared by cold rolling and spark erosion from a commercial 1 kg rectangular ingot of pure Sn with purity of 99.997%. The cold-rolled Sn plates were annealed at 473 K for 2 h in an oil bath with silicone oil and then chemically polished in an etchant composed of 25 vol% of hydrochloric acid and 75 vol% of distilled water. The two surfaces with an area of 12×5 mm^2 of each chemically polished plate were mechanically polished on 1000 emery paper. One of the two surfaces was again mechanically polished on 1500 emery paper until a depth of 100 μm and then finished using diamond with a diameter of 3 μm.

After chemically polishing, a Au sheet specimen was immediately sandwiched between two freshly prepared Sn plate specimens in methanol by a technique used in a previous study [6]. The Sn/Au/Sn couples were completely dried and then heat treated in the oil bath at 433 K for 1 h for diffusion bonding. The diffusion couples were annealed at 433 K for various times between 3 and 126 h. The summation of the heat-treating and annealing times is hereafter merely called the annealing time. Cross sections of the annealed diffusion couples were mechanically polished using diamond with diameters of 6, 3 and 1 μm, finished utilizing an OP-S liquid by Struers Ltd., and then chemically etched in an etchant consisting of 80 ml of ethanol, 20 ml of hydrochloric acid and 10 ml of nitric acid. The chemical etching was carried out for 30 s using the freshly prepared etchant. The microstructure of the cross section was observed with a differential interference contrast (DIC) optical microscope. Concentration profiles of Au and Sn were measured on the cross section along the direction normal to the interface by electron probe microanalysis (EPMA).

3. Results and discussion

3.1. Growth behavior of intermetallic layer

Typical DIC optical micrographs for the chemically etched cross-sections of the Sn/Au/Sn diffusion couples annealed at 433 K for 1 and 25 h are shown in Fig. 1a and b, respectively. As can be seen in these micrographs, orange and blue layers are observed to form at the Au/Sn interfaces. The thickness of the colored layer is about 8 and 30 μm in Fig. 1a and b, respectively. According to the micrograph in Fig. 1b, the layer seems to consist of various sub-layers with slightly different colors. In order to identify each sub-layer, concentration profiles of Au and Sn were determined by EPMA along the direction normal to the interface. A result of the determination for the diffusion couple annealed at 433 K for 127 h is plotted as open circles in Fig. 2. In this figure, the ordinate and the abscissa show the mol fraction of Au and the distance, respectively. According to the result in Fig. 2, three sub-layers with different stoichiometric compositions are discerned between the Au and Sn specimens. The first, second and third sub-layers from the Au side to the Sn side are AuSn, AuSn$_2$ and AuSn$_4$, respectively. The layer composed of these binary Au-Sn compound sub-layers is hereafter called the intermetallic layer. According to a recent phase diagram of the binary Au-Sn system [7], the Au$_5$Sn and ζ phases as well as the AuSn, AuSn$_2$ and AuSn$_4$ phases appear as stable intermetallic compounds at 433 K. However, the Au$_5$Sn and ζ phases are not recognized at the concentration profile in Fig. 2. The spatial resolution of EPMA is about 1 μm. Therefore, the compound sub-layer cannot be observed by EPMA, if its thickness is much smaller than the spatial resolution. This is the case for the Au$_5$Sn and ζ phases.

The reactive diffusion between Cu and Sn was experimentally examined by the present authors using a Sn/Cu/Sn diffusion couple [8]. The diffusion couple was prepared by a solid-state diffusion bonding technique and then annealed at 433 K for 120 h in the same oil bath as the present study. Under such conditions, a brittle oxide layer was observed to form at the interface in the Sn/Cu/Sn diffusion couple. Although the activity of oxygen is not determined at any locations of the silicone oil in the oil bath, the formation of the oxide layer implies that the annealing conditions are rather oxidative. Nevertheless, no oxide layer was recognized in the annealed Sn/Au/Sn diffusion couples. Consequently, we may expect that the binary Au-Sn intermetallic compounds are produced at the mechanically contacted interface between the Au-plated conductor and Sn-base solder alloys during energization

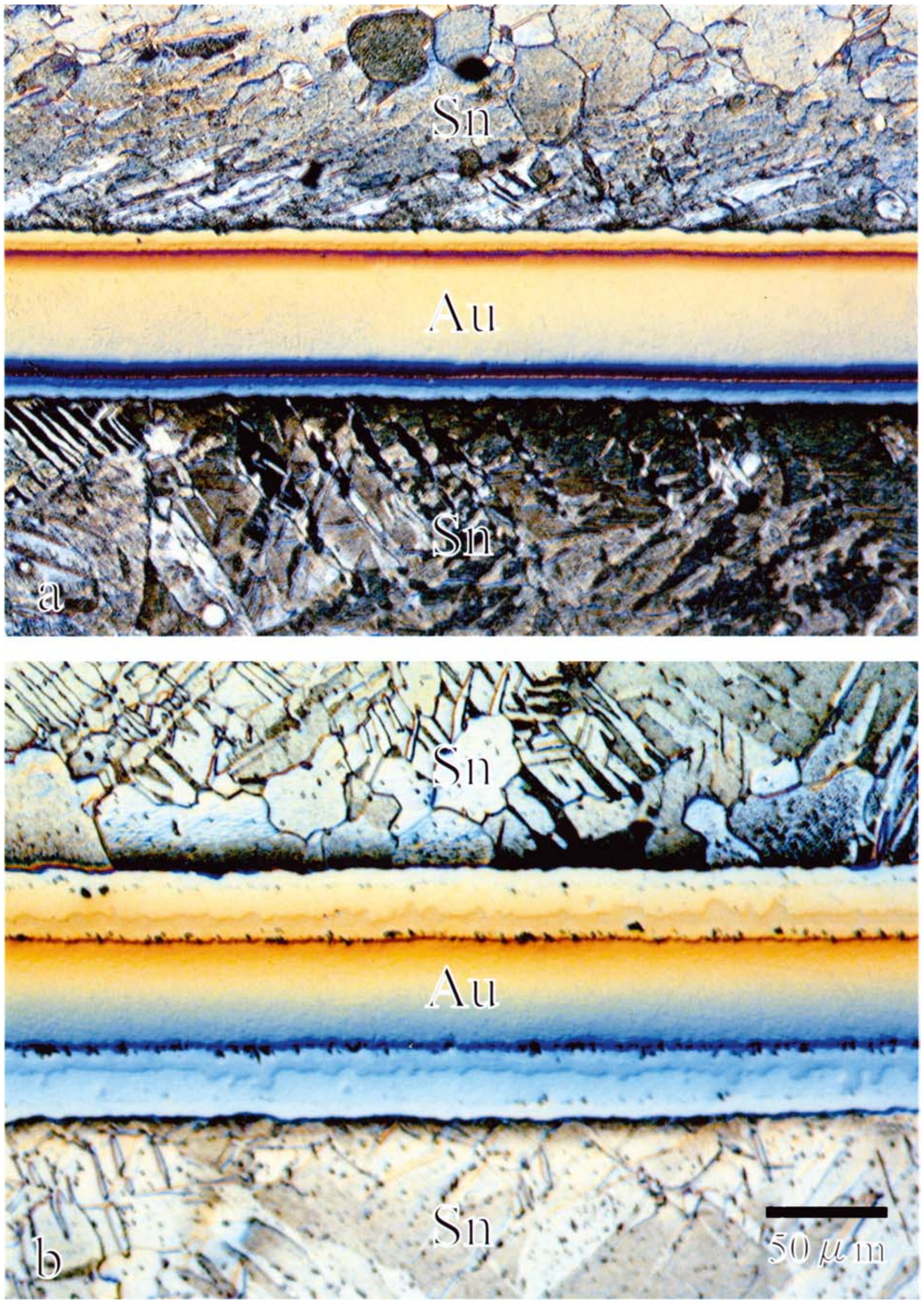

Figure 1 Optical micrographs of cross sections for the Sn/Au/Sn diffusion couples annealed at 433 K for: (a) 1 h (3.6×10^3 s) and (b) 25 h (9.0×10^4 s).

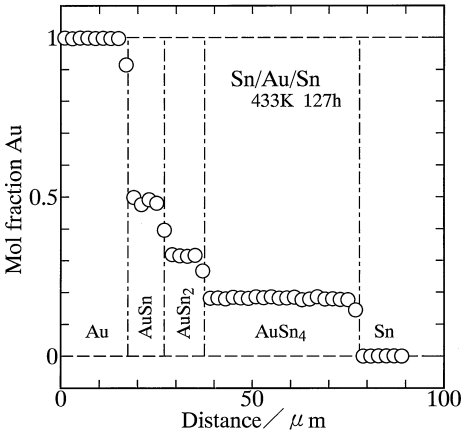

Figure 2 Concentration profile of Au across the colored layer in the Sn/Au/Sn diffusion couple annealed at 433 K for 127 h (4.57×10^5 s).

under usual service conditions unless the interface is completely exposed to air.

From the cross-sectional micrographs of the diffusion couples annealed at 433 K for various times, the average thickness l_i of layer i was evaluated by the following equation.

$$l_\mathrm{i} = A_\mathrm{i}/w_\mathrm{i} \tag{1}$$

Here, A_i and w_i are the total area and the total length of layer i, respectively, on the cross section. For convenience sake, the AuSn, $AuSn_2$ and $AuSn_4$ layers are denoted with subscripts of $i = 1$, 2 and 4, respectively. Although the AuSn layer is discriminated from the $AuSn_2$ layer in the concentration profile by EPMA, the interface between the AuSn and $AuSn_2$ layers is not so clearly distinguishable in the optical micrograph.

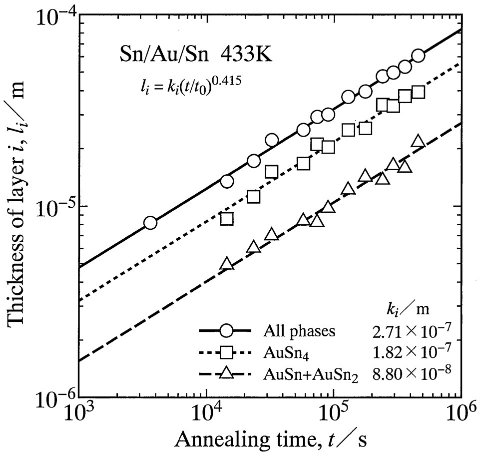

Figure 3 The thickness l_i of layer i versus the annealing time t for the Sn/Au/Sn diffusion couple annealed at 433 K. Straight lines indicate the calculations from Equation 2.

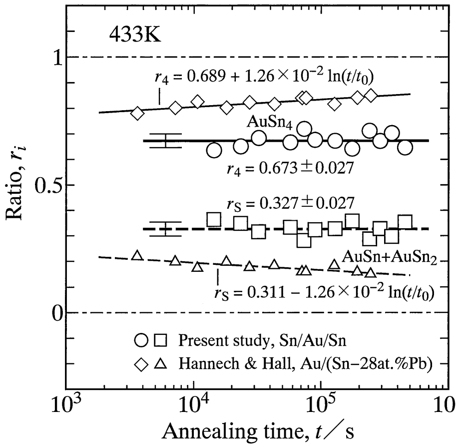

Figure 4 The ratio r_i versus the annealing time t for the Sn/Au/Sn diffusion couple annealed at 433 K. The results evaluated from the observations by Hannech and Hall for the Au/(Sn-Pb) diffusion couple [3] are also shown as open triangles and rhombuses.

Consequently, A_1 and A_2 could not be determined independently, and thus only the summation of l_1 and l_2 was evaluated. The thickness l_S is defined as the summation $l_S \equiv l_1 + l_2$, and the total thickness l of the intermetallic layer is obtained from the equation $l = l_4 + l_S$. The results for l, l_S and l_4 are shown as open circles, triangles and squares, respectively, in Fig. 3. In this figure, the ordinate indicates the logarithm of the thickness l_i, and the abscissa shows the logarithm of the annealing time t. As can be seen, the thicknesses l, l_S and l_4 monotonically increase with increasing annealing time t. Furthermore, the experimental points for each thickness are located well on a straight line. Therefore, l_i is described as a power function of t as follows.

$$l_i = k_i(t/t_0)^n \tag{2}$$

Here, t_0 is unity time, 1 s. It is adopted to make the ratio t/t_0 dimensionless. The proportionality coefficient k_i has the same dimension as the thickness l_i, but the exponent n is dimensionless. At each experimental annealing time, the ratio r_i of the thickness l_i to the total thickness l was calculated by the equation

$$r_i = l_i/l. \tag{3}$$

The results of r_4 and r_S are shown as open circles and squares, respectively, in Fig. 4. In this figure, the ordinate and the abscissa indicate the ratio r_i and the logarithm of the annealing time t, respectively. As can be seen, the ratios r_4 and r_S are almost constant independently of the annealing time, though the open circles and squares are slightly scattered. From these plotted points, the mean values are obtained to be 0.67 and 0.33 for r_4 and r_S, respectively. This means that the exponent n in Equation 2 takes the same value for the thicknesses l, l_S and l_4. Hence, the values of n and k_i were simultaneously determined by a least-squares method from all the plotted points in Fig. 3. The determination gives $k = 2.7 \times 10^{-7}$, $k_4 = 1.8 \times 10^{-7}$ and $k_S = 8.8 \times 10^{-8}$ m for l, l_4 and l_S, respectively, and $n = 0.42$. Using these parameters, the thickness l_i was calculated as a function of the annealing time t from Equation 2. The results are shown as parallel straight lines in Fig. 3. As can be seen, the experimental points for each thickness l_i lie well on the corresponding straight line.

Although the AuSn and $AuSn_2$ layers are not so clearly distinguishable each other in the optical micrograph as mentioned above, the concentration profile in Fig. 2 indicates that l_2 is almost equal to l_1. Therefore, we may consider that the ratio l_4:l_2:l_1 is nearly equivalent to 4:1:1. This ratio may be kept constant during annealing according to the results in Figs 3 and 4.

3.2. Comparison with results by soldering

As already mentioned in Introduction, Hannech and Hall experimentally observed the formation of the binary Au-Sn intermetallic compounds in the Au/(Sn-Pb) diffusion couple [3]. The diffusion couple was prepared by soldering a commercial flux-cored Sn-28 at% Pb alloy onto a thin Au layer electrodeposited on an alumina plate and then annealed at temperatures of 353 to 433 K. After soldering, the Sn-Pb alloy indicates the eutectic microstructure consisting of the α and β phases. Here, α and β stand for the primary solid solution phases of Sn and Pb, respectively. In the eutectic microstructure, the mean grain size is about 5 μm for both phases. The $AuSn_4$ layer was produced at the Au/(Sn-Pb) interface during soldering, and the $AuSn_2$ and AuSn layers were formed at the Au/$AuSn_4$ interface during annealing. In the ternary Au-Pb-Sn system [9], the Au_2Pb, $AuPb_2$ and $AuPb_3$ phases as well as the AuSn, $AuSn_2$ and $AuSn_4$ phases appear as stable binary intermetallic compounds at 433 K. No ternary intermetallic compound exists in this system. Although the ternary isothermal section at 433 K is not reported, the phase relationships imply the existence of the three-phase equilibria of $\alpha + \beta + AuSn_4$, $\beta + AuSn_4 + AuSn_2$ and $\beta + AuSn_2 + AuPb_3$ at this temperature [9]. However, no binary Au-Pb intermetallic compound was clearly recognized in the Au/(Sn-Pb) diffusion couple. During annealing, the α phase is reacted with Au to produce the AuSn, $AuSn_2$ and $AuSn_4$ compound layers, but the β phase remains in the

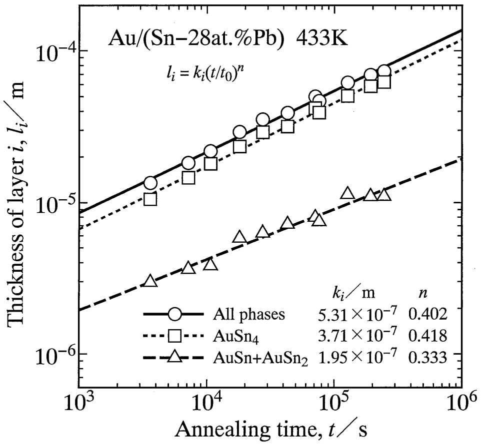

Figure 5 The thickness l_i of layer i versus the annealing time t for the Au/(Sn-Pb) diffusion couple annealed at 433 K by Hannech and Hall [3]. Straight lines indicate the calculations from Equation 2.

compound layers keeping the volume fraction almost constant. In their experiment, the annealing time dependence of the thickness was determined for the AuSn, AuSn$_2$ and AuSn$_4$ layers. The results are shown as open symbols in Fig. 5. Each open symbol in this figure indicates the same meaning as Fig. 3. According to the results in Fig. 5, the thickness l_i monotonically increases with increasing annealing time t. Also in this case, the plotted points for each thickness are located well on a straight line. This means that the annealing time dependence of the thickness is described by Equation 2. However, unlike Fig. 3, the straight lines are not parallel to one another. From the plotted points in Fig. 5, the ratio r_i was evaluated by Equation 3. The results for r_4 and r_S are shown as open rhombuses and triangles, respectively, in Fig. 4. As can be seen, r_4 is greater for the Au/(Sn-Pb) diffusion couple than for the Sn/Au/Sn diffusion couple, whereas r_S is smaller for the former diffusion couple than for the latter diffusion couple. In the Au/(Sn-Pb) diffusion couple, only the AuSn$_4$ layer was formed during soldering at 520 K, and then the AuSn and AuSn$_2$ layers were produced during annealing at 433 K. On the other hand, the AuSn, AuSn$_2$ and AuSn$_4$ layers were simultaneously formed during annealing at 433 K in the Sn/Au/Sn diffusion couple. The higher the temperature is, the larger the formation rate of the compound layer becomes. Hence, the AuSn$_4$ layer forms more rapidly during soldering at 520 K than during annealing at 433 K. This is the reason why r_4 is greater for the Au/(Sn-Pb) diffusion couple than for the Sn/Au/Sn diffusion couple. As the annealing time increases, r_4 slightly increases but r_S lightly decreases in the Au/(Sn-Pb) diffusion couple. Such annealing time dependencies of r_4 and r_S are expressed by the following equation.

$$r_i = a_i + b_i \ln(t/t_0) \qquad (4)$$

The parameters a_i and b_i in Equation 4 were determined by a least-squares method from the open rhombuses and triangles in Fig. 4. The determination reveals $a_4 = 0.69$ and $b_4 = 1.3 \times 10^{-2}$ for r_4 and $a_S = 0.31$ and $b_S = -1.3 \times 10^{-2}$ for r_S. As mentioned earlier, the straight lines in Fig. 5 are not parallel to one another. This means that the exponent n takes a different value for each thickness l_i. Hence, both parameters n and k_i in Equation 2 were independently evaluated by a least-squares method for each thickness l_i from the corresponding plotted points. The evaluation deduces $k = 5.3\times10^{-7}$ m and $n = 0.40$ for l, $k_4 = 3.7\times10^{-7}$ m and $n = 0.42$ for l_4, and $k_S = 2.0 \times 10^{-7}$ m and $n = 0.33$ for l_S. According to the phase equilibria reported for the ternary Au-Pb-Sn system [9], the β phase may be in equilibrium with the AuSn$_4$ and AuSn$_2$ phases but not with the AuSn phase at 433 K. As a consequence, during annealing, the β phase can penetrate into the AuSn$_4$ and AuSn$_2$ layers but should finally disappear in the AuSn layer. The growth behavior of the compound layers in the Au/(Sn-Pb) diffusion couple shown in Figs 4 and 5 might be relevant to such phase stability of the β phase. However, the information on the phase equilibria in the ternary Au-Pb-Sn system at 433 K is not enough to account for the growth behavior even qualitatively so far.

3.3. Rate-controlling process

The plotted points for the total thickness l in Figs 3 and 5 are represented as open circles and squares, respectively, in Fig. 6. As can be seen, l is greater for the Au/(Sn-Pb) diffusion couple than for the Sn/Au/Sn diffusion couple at each annealing time. Inserting the parameters $k = 5.3 \times 10^{-7}$ m and $n = 0.40$ into Equation 2, the total thickness is calculated to be $l = 8.5$, 22 and 54 μm at $t = 10^3$, 10^4 and 10^5 s, respectively, for the Au/(Sn-Pb) diffusion couple. On the other hand, the calculation with $k = 2.7 \times 10^{-7}$ m and $n = 0.42$ results in $l = 4.8$, 12 and 32 μm at $t = 10^3$, 10^4 and 10^5 s, respectively, for the Sn/Au/Sn diffusion couple. In the case of the Au/(Sn-Pb) diffusion couple, the AuSn$_4$ layer with a thickness of 2 μm was observed to form due to the reactive diffusion between the pure Au solid phase and the binary Sn-Pb liquid phase during soldering at 520 K [3]. Thus, the total thickness is expected to be always greater by 2 μm for the Au/(Sn-Pb) diffusion couple than for the

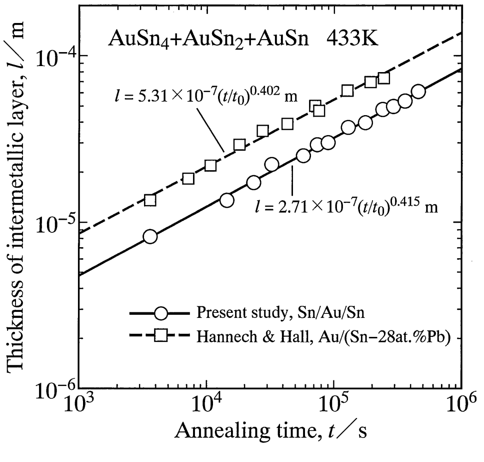

Figure 6 The total thickness l of the intermetallic layer versus the annealing time t for the Sn/Au/Sn and Au/(Sn-Pb) diffusion couples shown in Figs 3 and 5, respectively.

Sn/Au/Sn diffusion couple during annealing at 433 K unless the rate-controlling process varies. However, the difference of the total thickness between the Sn/Au/Sn and Au/(Sn-Pb) diffusion couples increases from 3.7 to 22 μm with increasing annealing time from $t = 10^3$ to 10^5 s.

The melting point is much lower for Sn and Pb than for Au [7, 9]. Therefore, at a constant temperature lower than the melting points of these elements, interdiffusion will take place faster in Sn and Pb than in Au. This implies that the interdiffusion in the Sn and Sn-Pb specimens plays the most important role for the growth of the intermetallic layer. As already mentioned in Section 3.2, the Sn-Pb specimen in the Au/(Sn-Pb) diffusion couple indicates the eutectic microstructure composed of the α and β phases with mean grain sizes of about 5 μm [3]. On the other hand, the mean grain size is about 20 μm for the Sn specimen in the Sn/Au/Sn diffusion couple. If the grain size is small, the grain boundary diffusion becomes predominant for the interdiffusion in a polycrystalline material. In order to estimate the contribution of the grain boundary diffusion to the interdiffusion, the effective diffusion coefficient D^{ef} is defined as

$$D^{\text{ef}} \equiv (1 - f^{\text{b}})D + f^{\text{b}}D^{\text{b}}. \tag{5}$$

Here, D and D^{b} are the interdiffusion coefficients for the volume diffusion and the grain boundary diffusion, respectively, and f^{b} is the fraction of the cross-sectional area of the grain boundary on the cross section vertical to the diffusion direction. If the shape of each grain in the Sn and Sn-Pb specimens is assumed to be rectangular, the fraction f^{b} is estimated by the equation

$$f^{\text{b}} = 2\delta/d, \tag{6}$$

where d is the length of the side for the rectangular grain, and δ is the thickness of the grain boundary. In the Au/(Sn-Pb) diffusion couple, the β phase remains in the intermetallic layer keeping the volume fraction almost constant during annealing. Therefore, the β phase may not play any important roles in the reactive diffusion. In order to estimate the value of D^{ef}, the eutectic Sn-Pb specimen can be treated as the polycrystalline Sn specimen with a mean grain size of 5 μm.

If the solution phase is dilute, the interdiffusion coefficient becomes nearly equal to the self-diffusion or tracer-diffusion coefficient of the solute [10]. According to the phase diagram in the binary Au-Sn system [7], the solubility of Au in Sn is less than 0.2 at% at 433 K. Hence, the α phase saturated with Au at 433 K is dilute enough to consider the self-diffusion coefficient of Au in Sn as the interdiffusion coefficient in the α phase. The temperature dependence is usually described as

$$D = D_0 \exp(-Q/RT) \tag{7}$$

and

$$s\delta D^{\text{b}} = s\delta D_0^{\text{b}} \exp(-Q^{\text{b}}/RT) \tag{8}$$

for the self-diffusion coefficient of the volume diffusion D and that of the grain boundary diffusion D^{b}, respectively. Here, D_0 and D_0^{b} are the pre-exponential factors, Q and Q^{b} are the activation enthalpies, s is the segregation coefficient of the solute in the grain boundary, R is the gas constant, and T is the absolute temperature. The self-diffusion coefficient for the volume diffusion of Au in Sn is reported at temperatures between 973 and 1273 K [11]. However, the information on the grain boundary diffusion of Au in Sn is not sufficient. On the contrary, the grain boundary diffusion of Ag in Sn was experimentally studied by Bartha at 340 to 422 K [12]. Adopting the parameters $D_0 = 1.18 \times 10^{-8}$ m^2/s and $Q = 58.83$ kJ/mol for the volume diffusion of Ag in Sn [13] and assuming $s = 1$ and $\delta = 5 \times 10^{-10}$ m, he determined values of $D_0^{\text{b}} = 3.9 \times 10^{-7}$ m^2/s and $Q^{\text{b}} = 28.16$ kJ/mol. The extrapolation with these parameters yields $D = 9.44 \times 10^{-16}$ m^2/s and $D^{\text{b}} = 1.56 \times 10^{-10}$ m^2/s at $T = 433$ K. If the value $\delta = 5 \times 10^{-10}$ m is used again, $f^{\text{b}} = 2 \times 10^{-4}$ and 5×10^{-5} are calculated for $d = 5$ and 20 μm, respectively, from Equation 6. Inserting those parameters into Equation 5, we finally obtain $D^{\text{ef}} = 3.22 \times 10^{-14}$ and 8.76 $\times 10^{-15}$ m^2/s for $d = 5$ and 20 μm, respectively. Hence, D^{ef} is 3.7 times greater for $d = 5$ μm than for $d = 20$ μm. This means that the interdiffusion takes place about four times faster in the Sn specimen with $d = 5$ μm than in that with $d = 20$ μm. Although this relationship has been drawn for the diffusion of Ag in the Sn specimen, similar grain-size dependence will exist also for the diffusion of Au in the Sn specimen. Consequently, we may conclude that the larger growth rate of the intermetallic layer in the Au/(Sn-Pb) diffusion couple than in the Sn/Au/Sn diffusion couple is owing to the faster interdiffusion in the Sn-Pb specimen than in the Sn specimen.

When the diffusion couple is initially composed of the specimens with semi-infinite thicknesses and the growth of the intermetallic layer is controlled by the volume diffusion in each phase, the exponent n in Equation 2 should be equal to 0.5. Such a relationship is called the parabolic relationship. However, the exponent n is 0.42 and 0.40 for the Sn/Au/Sn and Au/(Sn-Pb) diffusion couples, respectively, as shown in Fig. 6. In the case of the Au/(Sn-Pb) diffusion couple, the Sn-Pb alloy was soldered on the Au layer with a thickness of 12 μm [3]. After annealing at 433 K for 68 h, the Au layer was completely consumed to form the intermetallic layer with a thickness of 73 μm. This means that the Au/(Sn-Pb) diffusion couple is no longer the semi-infinite diffusion couple. In such a case, the parabolic relationship does not hold good, and thus the exponent n becomes smaller than 0.5. On the other hand, the Sn/Au/Sn diffusion couple consists of the Au sheet specimen with a thickness of 60 μm and the Sn plate specimens with a thickness of 2 mm. In this diffusion couple, the thicknesses of the Au specimen and the intermetallic layer become 40 and 61 μm, respectively, after annealing for 127 h at 433 K. The pre-exponential factor and the activation enthalpy of the self-diffusion coefficient D for the volume diffusion of Sn in Au are reported to be $D_0 = 4.1 \times 10^{-6}$ m^2/s and $Q = 143$ kJ/mol, respectively, at a temperature range between 973 and 1273 K

[11]. The extrapolation with these parameters provides $D = 2.3 \times 10^{-23}$ m^2/s at 433 K. Although the solubility of Sn in Au is not conclusively determined at temperatures lower than 673 K even in a recent phase diagram of the binary Au-Sn system [7], it should be smaller than 1 at% at 433 K according to the concentration profile in Fig. 2. Consequently, the Au (γ) phase saturated with Sn at 433 K is sufficiently dilute, and thus the interdiffusion coefficient for the volume diffusion in the γ phase is considered to be $D = 2.3 \times 10^{-23}$ m^2/s at 433 K. If the penetration distance x for the volume diffusion of Sn in the γ phase is roughly estimated by the equation $x^2 \cong 4\,Dt$, a value of $x = 6.5 \times 10^{-9}$ m is obtained for the longest experimental annealing time of $t = 4.57 \times 10^5$ s (127 h). This value of x is still four orders of magnitude smaller than the thickness of the Au specimen in the Sn/Au/Sn diffusion couple. On the other hand, the effective diffusion coefficient D^{ef} in the Sn specimen with $d = 20$ μm is obtained to be 8.76×10^{-15} m^2/s as mentioned above. Adopting this value, the penetration distance of Au in the Sn specimen is estimated to be $x = 1.3 \times 10^{-4}$ m for $t = 4.57 \times 10^5$ s (127 h). This value of x is merely 6% of the thickness of the Sn specimen. Hence, the Sn/Au/Sn diffusion couple is recognized to be the semi-infinite diffusion couple under the present annealing conditions. Nevertheless, the exponent n is slightly smaller than 0.5.

The reactive diffusion between the Ni and NiAl phases was experimentally studied by Nemoto and coworkers [14, 15]. In their experiment, the Ni/NiAl diffusion couples were prepared by a solid-state diffusion bonding technique and then annealed at temperatures between 1173 and 1523 K. During annealing, the Ni_3Al compound layer was observed to form at the Ni/NiAl interface. According to their observations, the annealing time dependence of the thickness l of the Ni_3Al layer is expressed by Equation 2. The exponent n is equal to 0.5 at 1373 to 1523 K, but becomes 0.25 at 1173 to 1273 K. Such growth behavior of the Ni_3Al layer due to the reactive diffusion is reported also by Janssen [16]. The value $n = 0.25$ indicates that the growth of the compound layer is controlled by the grain boundary diffusion [17]. The contribution g of the grain boundary diffusion to the interdiffusion in the Sn specimen of the Sn/Au/Sn diffusion couple is evaluated by the equation

$$g = f^{\mathrm{b}} D^{\mathrm{b}} / D^{\mathrm{ef}}. \tag{9}$$

Using the parameters for the diffusion of Ag in the Sn specimen with $d = 20$ μm, we obtain a value of $g = 0.89$ from Equation 9. This means that the interdiffusion in the Sn specimen is partially controlled by the grain boundary diffusion. Under such conditions, the exponent n will take a value between 0.25 and 0.5. However, it is worth repeating that the present evaluation has been carried out for the interdiffusion between Ag and Sn but not for that between Au and Sn. Hence, g may be different from 0.89 in the binary Au-Sn system.

As mentioned earlier, the Sn/Au/Sn diffusion couple is considered semi-infinite even at the longest annealing time, but the Au layer in the Au/(Sn-Pb) diffusion couple completely disappears after a certain annealing time. The disappearance of the Au layer decelerates the growth of the intermetallic layer. Nevertheless, the total thickness l is around 1.7 times greater for the Au/(Sn-Pb) diffusion couple than for the Sn/Au/Sn diffusion couple at the experimental annealing times. Such faster growth of the intermetallic layer in the former diffusion couple than in the latter diffusion couple is owing to the grain boundary diffusion in the Sn-Pb solder alloy with the fine-grain eutectic microstructure. In order to suppress the growth of the intermetallic layer, the fine-grain microstructure is not preferred for the Sn-base solder alloy. Such an effect of the microstructure on the kinetics of the reactive diffusion should be taken into account for estimation of the deterioration of the mechanical and electrical properties at the connection between the conductor and solder alloys.

4. Conclusions

In order to examine the kinetics of the reactive diffusion between Au and Sn, a solid-state diffusion bonding technique was adopted to prepare Sn/Au/Sn diffusion couples. The diffusion couples were annealed at 433 K for various times in the oil bath with silicone oil. After annealing, the AuSn, $AuSn_2$ and $AuSn_4$ compound layers were observed to form at the Au/Sn interface. The ratio of the thicknesses of the AuSn, $AuSn_2$ and $AuSn_4$ layers is nearly equal to 1:1:4 and kept constant during annealing. The total thickness l of the compound layer increases with annealing time t according to the relationship $l = k(t/t_0)^{\mathrm{n}}$, where t_0 is unity time, 1 s. The proportionality coefficient k and the exponent n were determined to be 2.7×10^{-7} m and 0.42, respectively, by a least-squares method on the basis of the observations. If the growth of the compound layers is controlled by the volume diffusion of the constituent elements, the thickness l should be proportional to the square root of the annealing time t. However, the exponent n is slightly smaller than 0.5. Therefore, the volume diffusion is not purely the rate-controlling process, but the grain boundary diffusion partially contributes to the growth of the compound layers. Such contribution of the grain boundary diffusion may be more remarkable for the reactive diffusion between the Sn-Pb solder alloy with the fine-grain eutectic microstructure and the Au layer plated on the Cu-base conductor alloy.

Acknowledgements

The authors are grateful to Professor Z. Horita with the Department of Materials Science and Engineering at Kyushu University, Japan for his helpful information on the reactive diffusion in the binary Ni-Al system. The present study was supported by Tyco Electronics AMP Co., Ltd., Japan.

References

1. H. N. KELLER, *IEEE Trans. Comp. Hybrids Manuf. Tech.* **CHMT-2** (1979) 180.
2. H. N. KELLER and J. M. MORABITO, *Surf. Interf. Anal.* **3** (1981) 16.

3. EI-B. HANNECH and C. R. HALL, *Mater. Sci. Tech.* **8** (1992) 817.
4. H. N. KELLER, *IEEE Trans. Comp. Hybrids Manuf. Tech.* **CHMT-5** (1982) 408.
5. C. WRIGHT, *IEEE Trans. Parts Hybrids Packaging* **PHP-13** (1977) 202.
6. Y. KAWANAMI, S. YOSHIDA, N. TAKEUCHI, M. KAJIHARA and T. MORI, *ISIJ Int.* **37** (1997) 596.
7. T. B. MASSALSKI, H. OKAMOTO, P. R. SUBRAMANIAN and L. KACPRZAK, "Binary Alloy Phase Diagrams," Vol. 1 (ASM Int., Materials Park, OH, 1990) p. 434.
8. T. YAMADA, "Master of Engineering Thesis" (Tokyo Institute of Technology, Tokyo, 2001).
9. G. EFFENBERG, F. ALDINGER and A. PRINCE, "Ternary Alloys," Vol. 13 (VCH Verlagsgesellschaft GmbH, Weinheim, 1995) p. 269.
10. L. DARKEN, *Trans. AIME* **174** (1948) 184.
11. "Metals Data Book," edited by Japan Inst. Metals (Marzen Co., Ltd., Tokyo, 1993) p. 20.
12. L. BARTHA, *Z. Metallknd.* **57** (1966) 482.
13. S. N. KRYUKOW and A. A. ZHUKOWITSKIJ, *Dokl. Akad. Nauk SSSR* **90** (1953) 379.
14. M. WATANABE, Z. HORITA and M. NEMOTO, *Interf. Sci.* **4** (1997) 229.
15. K. FUJIWARA, Z. HORITA and M. NEMOTO, in Proc. 3rd Pacific Rim Int. Conf. Adv. Mater. Proces (Min. Met. & Mater. Soc., 1998) p. 1251.
16. M. M. P. JANSSEN, *Metall. Trans.* **4** (1973) 1623.
17. Y. L. CORCORAN, A. H. KING, N. DE LANEROLLE and B. KIM, *J. Electr. Mater.* **19** (1990) 1177.

Received 2 July
and accepted 3 December 2003